analytical chemistry

Article

pubs.acs.org/ac

# Microchip Device with 64-Site Electrode Array for Multiplexed Immunoassay of Cell Surface Antigens Based on Electrochemiluminescence Resonance Energy Transfer

Mei-Sheng Wu, Hai-Wei Shi, Li-Jing He, Jing-Juan Xu,* and Hong-Yuan Chen

State Key Laboratory of Analytical Chemistry for Life Science, School of Chemistry and Chemical Engineering, Nanjing University, Nanjing 210093, China

Supporting Information

**ABSTRACT:** This paper describes a novel on-chip microarray platform based on an electrochemiluminescence resonance energy transfer (ECL-RET) strategy for rapid assay of cancer cell surface biomarkers. This platform consists of 64 antigen-decorated CdS nanorod spots with the diameter of 1.0 cm uniformly distributed on 16 indium tin oxide (ITO) strips, which is coated with a multichannel decorated polydimethylsiloxane (PDMS) slice to realize multiplexed determination of antigens. To shorten the immune reaction time in the microchannels and simplify the device, magnetic stirring and four-channel universal serial bus (USB) ports for plug-and-play were used. When $Ru(bpy)_3^{2+}$ labeled antibodies were selectively captured by the corresponding antigens on the CdS nanorod spot array, ECL-RET from the CdS nanorod (donor) by cathodic emission in the presence of $K_2S_2O_8$ to $Ru(bpy)_3^{2+}$ (acceptor) occurred. With signal amplification of $Ru(bpy)_3^{2+}$ and competitive immunoassay, carcinoembryonic antigen (CEA), $\alpha$-fetoprotein (AFP), and prostate specific antigen (PSA) as models were detected on this microfluidic device via recording the increased ECL-RET signals on electrode surfaces. Furthermore, this multiplexed competitive immunoassay was successfully used for detecting cancer cell surface antigens via the specific antibody–cell interactions and cell counting via cell surface receptors and antigens on the CdS nanorod surface. This platform provides a rapid and simple but sensitive approach with microliter-level sample volume and holds great promise for multiplexed detection of antigens and antigen-specific cells.

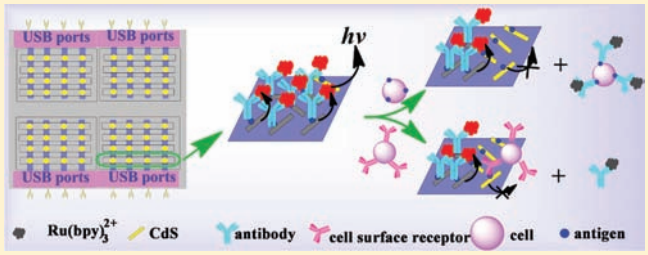


Tumor biomarkers are substances that can be found in the body when cancer is present and whose identification and measurement holds significant promise for the early detection of cancer and therapy monitoring.[1−3] Since carcinogenesis is a complicated process and most cancers have more than one marker associated with their incidence, the measurement of a single tumor marker is usually not sufficient to diagnose cancer.[4] Thus, sensitive, precise, and accurate multianalyte assays for measuring tumor markers in biological samples will be valuable tools in a wide range of clinical applications.

There has been considerable effort in recent years to develop multianalyte immunoassays including fluorescence immunoassay[5,6] and electrochemical immunoassay[7−9] based on multiple labels to realize simultaneous multianalyte determination. Compared with these immunoassays, the development of multianalyte assays based on other detection strategies such as electrochemiluminescence (ECL) is rare. ECL, which has been widely applied in bioanalytical applications, combines the analytical advantages of chemiluminescent analysis with electrochemical assay such as low background, specificity of ECL reaction, simple instrumentation, and low cost. The most common system used for analytical purposes consists of the luminophore label $Ru(bpy)_3^{2+}$ with tri-n-propylamine (TPrA) as a coreactant, for the reason that $Ru(bpy)_3^{2+}$ has high quantum yields and long excited state lifetimes as well as strong luminescence.[10−13] Recently, Walt and Rusling described a microwell array based ECL biosensor for the simultaneous detection of multiple species using $Ru(bpy)_3^{2+}$ as ECL emitter.[14,15]

Here, we report an ECL immunoassay for the simultaneous measurements of multiple proteins based on the use of CdS nanorod spots. ECL from semiconductor nanocrystals (S-NCs) has attracted a growing interest in biological/chemical analysis since ECL from Si NCs was first observed.[16] The diversity and tunable sizes of S-NCs result in tunable emission wavelength, which greatly increases their applications in bioanalysis based on ECL resonance energy transfer (ECL-RET), for it is easy to find suitable spectra overlapped pairs of donor–acceptor. Since no external light source is used for excitation in ECL-RET approaches, background noise caused by the direct excitation of the acceptor as often observed in fluorescence resonance energy transfer (FRET) can be avoided. Besides, ECL donor can be immobilized on electrode surface which gives an enhanced ECL signal. It has been proved that the ECL-RET

**Received:** February 27, 2012
**Accepted:** April 10, 2012
**Published:** April 10, 2012

   dx.doi.org/10.1021/ac300551e | *Anal. Chem.* 2012, 84, 4207−4213

**Scheme 1. (A) Layout of the Microchip for Multiplexed Immunoassay, (B) Layout of Four Spots in One Microchannel, and (C) Principle of Competitive ECL-RET Process in Determination of Antigen Specific Cells and Receptor Specific Cells[a]**

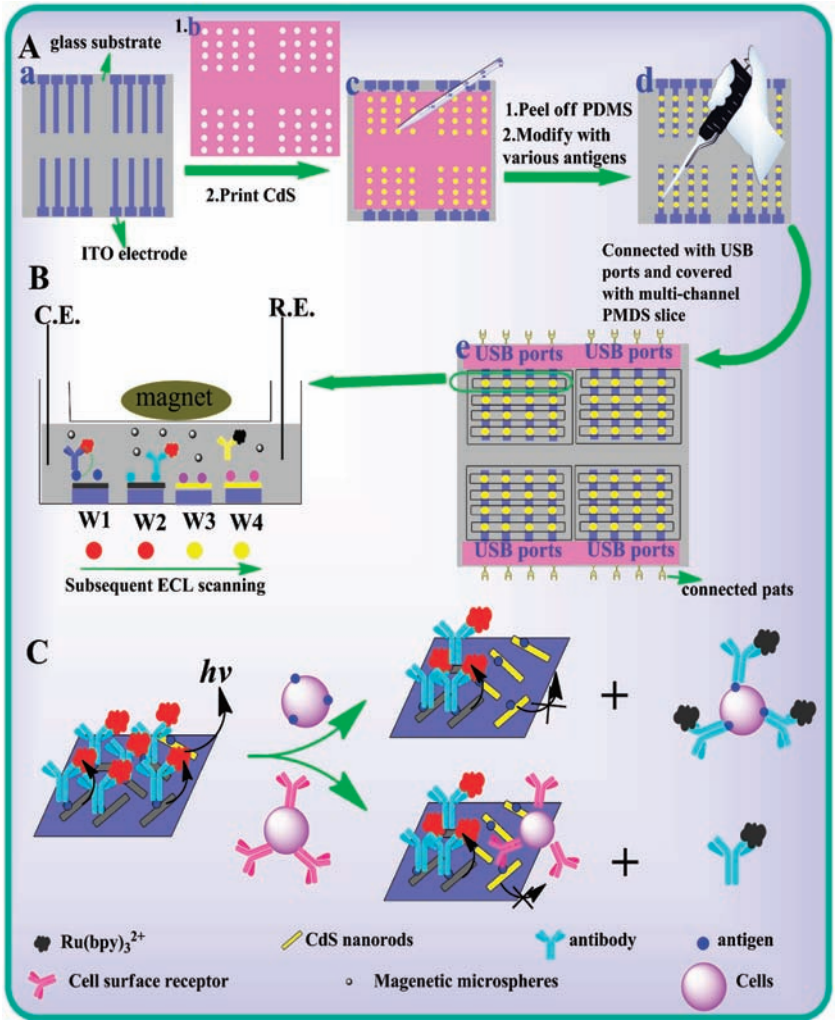


[a]For A, (a) four groups of ITO strips on glass substrate; (b) a 64-site PDMS reservoir array; (c) binding b on a, then printing CdS nanorods to the PDMS reservoirs; (d) removing the PDMS reservoir array and immobilizing various antigens on CdS nanorod spots; (e) binding a multi-channel PDMS slice on the CdS nanorod patterned glass substrate. A four-channel USB port was connected with ITO electrode for plug-and-play. The counter electrode and reference electrode were situated at the two ends of the channels. For B, ITO strips were numbered from left to right (W1 to W4) on each group. The external magnet was used to control magnetic microspheres in the channels to perform rapid mixing.

approach is very efficient in biosensing[17−20] and monitoring molecular interactions.[21] For example, in a recently published communication, we reported an ECL-RET protocol involving energy transfer from an ECL donor (CdS quantum dots (QDs)) to an acceptor ($Ru(bpy)_3^{2+}$). No cathodic ECL emission of $Ru(bpy)_3^{2+}$ in the potential range from 0 to −1.4 V vs SCE (saturated calomel electrode) makes it a sensitive energy acceptor of cathodic ECL donor with interference free from its own ECL emission.[20] In this system, $Ru(bpy)_3^{2+}$ labeled SMMC-7721 cell was captured from solution by anti-$\beta$2 microglobulin antibodies on CdS QD modified glassy carbon electrode, leading to CdS QDs and $Ru(bpy)_3^{2+}$ being closer together and making ECL-RET occur.

In this work, we presented a novel on-chip microarray platform based on ECL-RET strategy for rapid and multiplexed assay of cancer cell biomarkers. This platform consisted of a 64-site electrode array, which was covered with a multichannel decorated polydimethylsiloxane (PDMS) slice. An indium tin oxide (ITO) strip array was fabricated with a PDMS micromold while using carbon ink as a protective layer in place of a traditional photoresist design.[22] Magnetic stirring was used for accelerating the immune reaction via adding magnetic nanoparticles in channels which were controlled by an external magnet. Four-channel universal serial bus (USB) ports were used to realize plug-and-play which facilitate the multiplexed measurement. To achieve a facile approach to detect multiple antigens, antigens were preimmobilized on CdS nanorod spots to selectively capture the corresponding $Ru(bpy)_3^{2+}$ (energy acceptor) labeled antibodies. With the proceeding of the immune reaction, the $Ru(bpy)_3^{2+}$ labeled antibody was captured on CdS/antigen surface and caused the ECL emission color transformation from green (CdS nanorod) to red ($Ru(bpy)_3^{2+}$) gradually. This platform was further exploited to identify and detect cell surface specific proteins in a complex matrix based on the competitive ECL-RET immunoassay. The results show that this microchip device presents great promise for rapid and sensitive determination of cell surface biomarkers.


dx.doi.org/10.1021/ac300551e | Anal. Chem. 2012, 84, 4207−4213

## EXPERIMENTAL SECTION

Chemicals, materials, and the apparatus are presented in the Supporting Information.

**Fabrication of CdS Nanorod Patterned ITO Strip Array.** Scheme 1 schematically described the procedures for preparation of the CdS nanorod spot array with a 64-site PDMS reservoir array (1 mm diameter and 1.5 mm depth). The details for preparing CdS nanorods and the ITO strip array are shown in the Supporting Information. The ITO strip array with 4 groups was covered by the PDMS reservoir array with all the reservoirs on ITO strips and filled with 0.5 mg/mL CdS nanorods as the "ink" for the printing spot array. Here, the PDMS reservoir array was used to maintain the position of the CdS nanorod on ITO strips, facilitating the immobilization of multiple spots and avoiding the diffusion problem during drop-casting. This step was repeated until the desired number of the CdS nanorod layer was obtained. After that, the PDMS reservoir array was removed, and the prepared CdS nanorod spot array was displayed in Scheme 1A-d.

**Fabrication of Multiplexed Immunoassay Interface and Multiplexed Immunoassay Device.** To fabricate a multiplexed immunoassay interface, antigens with different concentrations were spotted onto the CdS nanorod surface. The details for fabrication multiplexed immunoassay interface are shown in the Supporting Information. The spatial separation between antigens enabled an individual immunoassay to be performed at each spot without interference due to diffusion crosstalk.

To fabricate the microfluidic multiplexed immunoassay device, the substrate with multiplexed immunoassay interface was reversibly bonded to a multichannel PDMS slice with the channels perpendicular to the ITO strips and the immunosensing surfaces in the channels. Then, one group of ITO strips was connected with a four-channel USB port to realize plug-and-play detection. This device contained 16 microchannels with four CdS nanorod spots in each microchannel (1.0 mm diameter). Ag/AgCl and Pt wire were placed at the two ends of each microchannel and used as reference and auxiliary electrodes, respectively. Thus, each spot can be used as a working electrode, and 64 individual analyses could be performed on one chip (Scheme 1A-e).

**Procedure for ECL-RET Assay.** An ECL-RET immunoassay was conducted for the detection of multiplexed antigens. At the start of the experiment, $\alpha$-fetoprotein (AFP), carcinoembryonic antigen (CEA), and prostate specific antigen (PSA) standard solutions were patterned on the CdS nanorod spot array to fabricate the immunoassay interfaces as described above. The antigen/CdS nanorod interfaces were blocked with 5% bovine serum albumin (BSA) solution and incubated with 30 $\mu$L of 50 $\mu$g/mL AFP antibody, CEA antibody, and PSA antibody labeled with $Ru(bpy)_3^{2+}$ in a 0.1 M $Na_2B_4O_7$–$H_3BO_3$ buffer solution (pH 7.4, containing 50 mM $K_2S_2O_8$ and 38.5 mg/L $Fe_3O_4$ magnetic microspheres) under magnetic stirring with an external magnet for 10 min. Details of preparing magnetic beads and $Ru(bpy)_3^{2+}$ labeled antibodies were shown in the Supporting Information. After washing with $Na_2B_4O_7$–$H_3BO_3$ buffer solution, the microchannel was filled with detection solution, and a cyclic potential sweep from −0.4 to −1.55 V was applied on the four-channel USB port. ECL spectra were monitored with an MPI-E multifunctional electrochemical and chemiluminescent analytical system by optical filters from 440 to 660 nm. For quantitative measurement, the ECL signals were recorded at the maximum emission wavelength of $Ru(bpy)_3^{2+}$ (620 nm).

Moreover, this device was further used to identify and detect cell surface specific antigens in a complex matrix with the competitive ECL-RET strategy (Scheme 1C). SMMC-7721 cells, MCF-7 cells, and PC-3 cells in 0.1 M phosphate-buffered saline (PBS, pH 7.4, containing 137 mM NaCl, 2.7 mM KCl, 87.2 mM $Na_2HPO_4$, and 14.1 mM $KH_2PO_4$) and 38.5 mg/L $Fe_3O_4$ magnetic microspheres were introduced into the as-prepared ECL-RET system under magnetic stirring. Finally, the microchannels were washed three times with PBS, and ECL-RET signals were obtained as a function of cell number.

## RESULTS AND DISCUSSION

**Characterization of CdS Nanorod Printed Electrodes Array.** For this array detector, the key element is the reproducibility of the CdS nanorod printed electrode array. First, we used transmission electron microscopy (TEM) and scanning electron microscopy (SEM) to characterize the morphology of the as-prepared CdS nanorods (Figure S1 in Supporting Information). The typical TEM image in Figure S1A (Supporting Information) revealed the average diameter of CdS nanorods was ca. 3.3 nm and their size distribution is relatively uniform. The SEM image showed that the multilayered CdS nanorods displayed an aggregated structure on the ITO electrode (Figure S1B, Supporting Information). From the amplified image (inset in Figure S1B, Supporting Information), we can see that the aggregated structure is composed of many nanorods. After the immobilization of antigen/antibody, all of the CdS nanorods were covered by these biomolecules and the film became smooth (Figure S1C, Supporting Information), indicating the successful attachment of antibody/antigen on the CdS nanorod spot array.

Figure 1A showed a typical optical image of a 16 element CdS nanorod spot array with the diameter of 1002 ± 28 $\mu$m (RSD = 2.8%) on the ITO strip array (1010 $\mu$m width for a single strip). Both the ITO strip array and CdS nanorod spot array displayed good shape and homogeneity. To gain a better understanding of ECL generation, cyclic voltammograms (CV, Figure 1B) and ECL-potential curves (inset of Figure 1B) of CdS nanorods in the presence (a) and absence (b) of $K_2S_2O_8$ were investigated. In the absence of $K_2S_2O_8$, a pair of small reduction and oxidation peaks appeared at ca. −1.40 V (C) and −1.10 V (A), which corresponded to the redox of CdS nanorods (Figure 1B, curve b). In the presence of $K_2S_2O_8$, a significantly increased reduction current was observed compared to that without $K_2S_2O_8$ due to the coreduction of $K_2S_2O_8$ on the ITO electrode (Figure 1B, curve a). As can be seen in the inset of Figure 1B, a strong ECL is produced upon concomitant reduction of CdS nanorods and $S_2O_8^{2-}$. When the potential was scanned in the negative direction, CdS nanorods on the electrode surface were reduced to $CdS^{-\bullet}$, and the coreactant $S_2O_8^{2-}$ was reduced to the strong oxidant $SO_4^{-\bullet}$. Then, $CdS^{-\bullet}$ could react with $SO_4^{-\bullet}$ through electron transfer to lead to the excited state (CdS*), which emits light. The corresponding ECL process is as follows:[17]

$$CdS + ne^- \rightarrow nCdS^{-\bullet} \quad (1)$$

$$S_2O_8^{2-} + e^- \rightarrow SO_4^{2-} + SO_4^{-\bullet} \quad (2)$$

$$CdS^{-\bullet} + SO_4^{-\bullet} \rightarrow CdS^* + SO_4^{2-} \quad (3)$$

$$CdS^* \rightarrow h\nu + CdS \quad (4)$$


dx.doi.org/10.1021/ac300551e | Anal. Chem. 2012, 84, 4207–4213

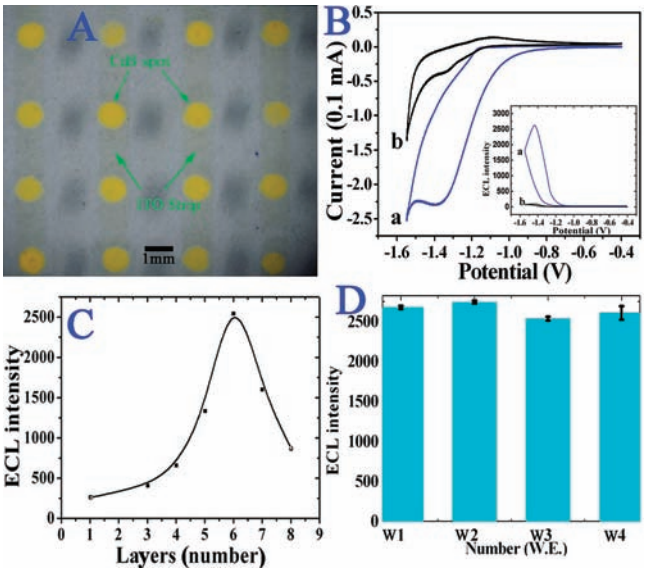


**Figure 1.** (A) Optical micrograph of the 16 element CdS nanorod spot array on ITO strips. (B) Typical cyclic voltammogram of one of the CdS nanorod modified ITO spots in 0.1 M $Na_2B_4O_7$–$H_3BO_3$ buffer solution (pH 7.4) with (a) and without (b) 50 mM $K_2S_2O_8$; inset was the corresponding ECL-potential curve of CdS nanorods with (a) and without (b) 50 mM $K_2S_2O_8$. (C) The effect of the number of the CdS nanorod layer on ECL intensity (from 1 to 8). (D) ECL intensity of CdS nanorod (3.3 nm) spots on one group of ITO strips (each strip with four spots). PMT was set at 600 V.

It is obvious that the ECL signal will increase with the increase of the amount of CdS nanorods on each spot. However, too thick of a CdS nanorod film could block the electron exchange of coreactant ($K_2S_2O_8$) with the electrode; meanwhile, the transparency of the CdS nanorod modified ITO electrode would become worse, both of which would result in a decrease of ECL signal. In order to obtain strong ECL emission film, we optimized the number of the CdS nanorod layer for ECL detection. As depicted in Figure 1C, the ECL intensity increases as the number of CdS layers increases from 1 to 6. When the number of CdS layers exceeds 6, the ECL response decreases. Therefore, the optimal assembly number of the CdS nanorod layer is 6. Under continuously cyclic potential scanning (in Figure S2 of Supporting Information), this multilayered CdS nanorod film displayed a stable, strong, and reproducible ECL emission which suggested that this mini on-chip immunoarray was suitable for the ECL assay. Before proceeding to the multiplex immunoassay, the spot-to-spot reproducibility of ECL on the array should be evaluated. As shown in Figure 1D, immunoassays for AFP on each ITO strip with four spots had good reproducibility, the relative standard deviations (RSD%, $n$ = 4) for the four strips were 0.7%, 0.7%, 1.0%, and 3.2%, respectively. The total RSD% of 16 spots was 3.5% ($n$ = 16). These results indicated that the CdS nanorod patterned ITO strip array possessed good stability and reproducibility which ensured high-throughput scanning of several cancer biomarkers simultaneously.

**On-Chip ECL-RET Immunoassay.** ECL-RET has been proved to be a sensitive strategy due to the low background and the high molar extinction coefficient[20] of ECL acceptor ($Ru(bpy)_3^{2+}$) and the tunable emission wavelength of ECL donor (CdS nanorod). The multiplexed assay for antigens was based on ECL-RET between the donor array and the acceptor in microfluidic chip, shown in Scheme 1B–C. When Ru-$(bpy)_3^{2+}$ labeled antibodies were captured by their corresponding antigens at the CdS nanorod region, ECL-RET could take place between them. The size of the CdS nanorods for the assay was selected to make the emission spectrum overlap well with the absorption spectrum of $Ru(bpy)_3^{2+}$. Figure S3 in the Supporting Information presented the absorption spectrum of $Ru(bpy)_3^{2+}$ and ECL emission spectra of CdS nanorods with different sizes. The emission peaks were at 460, 480, and 500 nm for 2.4, 3.3, and 3.6 nm CdS, respectively. The absorption spectrum of $Ru(bpy)_3^{2+}$ showed a peak centered at 465 nm (inset in Figure S3, Supporting Information), and it demonstrated a huge spectral overlap with the emission spectra of 2.4 and 3.3 nm CdS nanorods. While 3.3 nm CdS showed a higher ECL quantum yield than that of 2.4 nm CdS, it would be expected to result in a higher ECL-RET efficiency. Hence, 3.3 nm CdS was chosen for further ECL-RET assays.

To examine the applicability of ECL-RET on the microfluidic immunoassay, we studied the ECL responses of CdS nanorod and $Ru(bpy)_3^{2+}$ at different wavelengths on the ITO electrode surface. Figure 2 showed the ECL spectra of CdS nanorod/

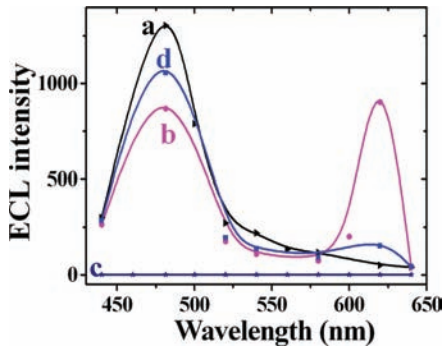


**Figure 2.** Emission spectra of 3.3 nm CdS nanorod/AFP before (a) and after (b) incubation in 50 $\mu$g/mL $Ru(bpy)_3^{2+}$ labeled anti-AFP antibody; (c) ECL emission of 50 $\mu$g/mL $Ru(bpy)_3^{2+}$ labeled anti-AFP antibody on bare ITO electrode; (d) ECL emission of b after incubating with $3 \times 10^4$ SMMC-7721 cells. Potential scan was from −0.4 to −1.55 V. The ECL spectra were recorded by optical filters from 440 to 660 nm. PMT was set at 800 V. ECL detection buffer: 0.1 M $Na_2B_4O_7$–$H_3BO_3$ buffer solution (pH 7.4) containing 50 mM $K_2S_2O_8$.

antigen in the absence and presence of $Ru(bpy)_3^{2+}$/antibody. When $Ru(bpy)_3^{2+}$/antibody was captured by antigen on the CdS nanorod, the donor's ECL emission at 480 nm (curves a and b) decreased and a new emission peak emerged at 620 nm. Furthermore, when applying the cyclic potential scan on the bare ITO electrode with $Ru(bpy)_3^{2+}$ labeled anti-AFP antibody, no cathodic ECL emission occurred (curve c), which implied that the newly emerged ECL peak at 620 nm (curve b) attributed to the emission of $Ru(bpy)_3^{2+}$ by the RET process and the ECL intensity caused by $Ru(bpy)_3^{2+}$ alone can be neglected. The increment of ECL at 620 nm was larger than the decrement of ECL at 480 nm, indicating that the signal could be amplified via ECL-RET.

As we know, an immunoassay usually needs a long incubation time due to the slow diffusion of analyte through an unstirred layer to form the immunocomplex. Figure S4 (curve a), Supporting Information, showed the dependence of the ECL response of an AFP/anti-AFP antibody system at 620 nm on the incubation time under the state of rest. With the increase of incubation time, the ECL response gradually


dx.doi.org/10.1021/ac300551e | Anal. Chem. 2012, 84, 4207–4213

increased and reached a plateau at 33 min. In order to accelerate the immunoreaction, magnetic stirring was applied via adding magnetic nanoparticles in channels which were controlled by an external magnet. As expected, an obvious different ECL signal path was obtained in Figure S4, curve b, Supporting Information. In the presence of magnetic stirring, the ECL-RET signal reached its plateau much faster than that of only molecular diffusion and immune reaction was completed within 7 min. Both cases showed the same plateau level, indicating that there was no nonspecific adsorption of proteins on the surface of magnetic microspheres. It was further confirmed by a UV−vis absorption spectrum of the magnetic microspheres after incubating with albumin fluorescein isothiocyanate (FITC-HAS) for 2 h and then washing with PBS three times (Figure S5, Supporting Information).

**Analytical Performance.** Due to its high-throughput, the microarray chip has been developed for protein assay[23−26] and probing the carbohydrate−protein interactions with DNA microarrays.[27] The aim of this work was to fabricate a mini on-chip multiplexed immunoassay by arraying various antigens on CdS nanorod spots. By varying the concentration of antigens on CdS nanorod spots from ng/mL to $\mu$g/mL and giving a constant spotting solution volume of antigens at 0.5 $\mu$L, the lowest amount of antigens that can be detected is on the order of pg.

Three kinds of antigens (AFP, CEA, and PSA) with various concentrations were spotted on CdS nanorods for multiplexed detection. The obtained ECL-RET response for AFP, CEA, and PSA were presented in Figure S6A−C, Supporting Information. Upon adding the corresponding $Ru(bpy)_3^{2+}$/antibody to microchannels, the ECL signal showed an increment at 620 nm with the increase of antigen concentrations. All the results demonstrated good linear relationships between acceptor's emission and the logarithm of antigens concentration in the ranges of 0.75 ng/mL to 75 ng/mL for AFP (A), 0.57 ng/mL to 0.50 $\mu$g/mL for CEA (B), and 1.0 ng/mL to 1.25 $\mu$g/mL for PSA (C). The linear calibration curves were $ECL_{620\ nm}$ = 325.91 + 845.88 log C (AFP, ng/mL, RSD = 0.995), $ECL_{620\ nm}$ = 556.78 + 534.00 log C (CEA, ng/mL, RSD= 0.992), and $ECL_{620\ nm}$ = 55.12 + 476.24 log C (PSA, ng/mL, RSD = 0.990), respectively. Since the threshold value in normal human serum is ∼10 ng/mL for AFP, ∼4 ng/mL for CEA, and ∼4 ng/mL for PSA, this multiplexed immunoassay could completely meet the requirements of clinical diagnosis.

The control experiments used the AFP array in the presence of $Ru(bpy)_3^{2+}$/AFP antibody, $Ru(bpy)_3^{2+}$/CEA antibody, and $Ru(bpy)_3^{2+}$/PSA antibody to test the selectivity of this on-chip multiplexed ECL immunoassay, shown in Figure S6 D, Supporting Information. It could be observed that AFP spots led to evident ECL-RET changes for $Ru(bpy)_3^{2+}$/AFP antibody, while there were no remarkable ECL-RET changes for $Ru(bpy)_3^{2+}$/CEA antibody and $Ru(bpy)_3^{2+}$/PSA antibody. It indicated that the proposed strategy possessed good selectivity for multiplexed detection, which was able to distinguish targets in a complex matrix.

**Multiplexed Cells Identification and Detection.** Since we had already detected several antigens simultaneously within this device, a scheme that incorporated these antigen arrays at different regions would extend this platform for multiplexed cancer cell detection and identification in a complex matrix by a competitive ECL-RET immunoassay.[28] To evaluate whether this strategy could be further used for cell analysis, we first studied the cytotoxicity of CdS nanorods by incubating them with SMMC-7721 cells in a 6-well cell culture plate in a $CO_2$ incubator (37 °C, 5% $CO_2$). It demonstrated that CdS nanorods displayed no obvious cytotoxicity during 24 h (Figure S7, Supporting Information). Thereafter, we investigated the possible competitive ECL-RET mechanism for cell analysis. Scheme 1C shows two different competitive recognition mechanisms for cancer cells. One is between cell surface antigens and $Ru(bpy)_3^{2+}$ labeled antibodies, and the other one is between cell surface receptors and antigens on the CdS nanorod surface. The former is caused by the competitive binding of cell surface antigens to $Ru(bpy)_3^{2+}$/antibodies and formed immunocomplex in solution, while the latter is caused by the specific conjugation of cell surface receptor with antigens on CdS nanorods, forming an immunocomplex at the electrode surface which results in an additional inhibition of the donor's ECL emission. In both recognition events, cells were employed to separate the donor and acceptor by competitive immunoassay. As a result, ECL-RET from the donor to the acceptor will decrease when cells are introduced into the system, enabling the identification and quantification of cells by immunoreaction.

As proof-of-principle of the competitive strategy, SMMC-7721 cells were used to testify the cells identification capability of this device. SMMC-7721 cells were introduced into the microchannel to bind with the $Ru(bpy)_3^{2+}$/AFP-antibody on AFP modified CdS nanorod spots. The competitive immunoassay was confirmed by the ECL spectra before and after cell incubation, shown in Figure 2 (curve b and d). Upon the proceeding of competitive immunoreaction, ECL-RET decreased in a cell concentration-dependent manner with the recovery of ECL emission of the CdS nanorod at 480 nm and the decrement emission of the acceptor at 620 nm, which confirmed that this mini on-chip device can be further used for determination of antigen specific cells.

Efficient identification of target cells is a prerequisite for a reliable and specific multiplexed method. First, one group of ITO strip array, which consisted of 16 identical CdS nanorod spots on four ITO strips, was used as an array detector. Antigen (AFP, CEA, and PSA) with four copies was spotted on four CdS nanorod spots of ITO strips (W1−W3), respectively. W4 was acting as a negative control. $Ru(bpy)_3^{2+}$/antibodies were then captured by the corresponding antigens at different locations on the microarray to form the ECL-RET system. SMMC-7721 cells (low expression of AFP[29]), MCF-7 cells (AFP receptor positive[30] and CEA positive[31]), PC-3 cells (PSA negative[32]), and a mixture of the three cell lines were then introduced into different microchannels and incubated with an antibody−antigen spot array. The ECL data at 620 nm were recorded depending on different cell lines, as shown in Figure 3. Changes of ECL signal represented the selectivity of an antigen−antibody spot on each cancer cell or an increasing population of a particular cancer cell type that expresses the antigen or receptor. The results from Figure 3 revealed that delivery of SMMC-7721 resulted in ECL changes only at AFP spots by the conjugation between cell surface AFP and $Ru(bpy)_3^{2+}$/AFP-antibody. For MCF-7 cells, they yielded ECL changes at both AFP spots and CEA spots with different competitive immunoreaction processes. The ECL change for MCF-7 cells at CEA spots was caused by the conjugation between cell surface CEA and $Ru(bpy)_3^{2+}$/CEA-antibody, while at AFP spots it is attributed to the combination of cell surface AFP receptors and CdS nanorod/AFP antigen spots. For PC-3 cells, it showed no ECL changes at the three antigen spot array.


dx.doi.org/10.1021/ac300551e | Anal. Chem. 2012, 84, 4207−4213

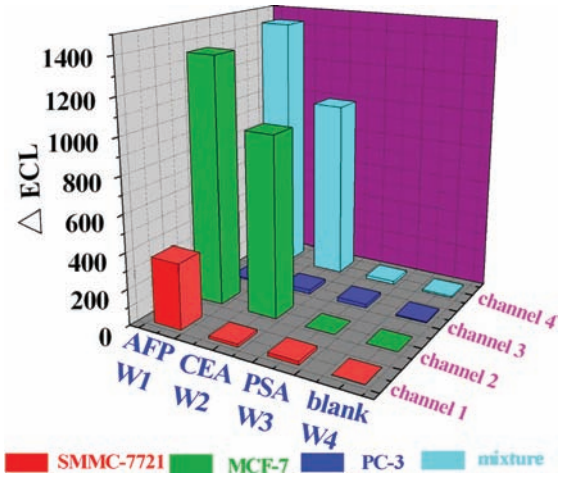


**Figure 3.** ECL-RET response of cell surface antigens in a complex matrix. AFP, CEA, and PSA were spotted on ITO strips from W1–W3, respectively. W4 was used as a negative control. Each strip contains 4 replicate antigen decorated CdS nanorod spots. After being captured by the corresponding $Ru(bpy)_3^{2+}$/antibody, SMMC-7721 cells ($6.0 \times 10^3$), MCF-7 cells ($6.4 \times 10^3$), PC-3 cells ($6.1 \times 10^3$), and mixed cells (SMMC-7721, MCF-7 cells, and PC-3 cells) were introduced in channel 1 to 4, respectively. ECL-RET signals were recorded at 620 nm. PMT was set at 800 V. ECL detection buffer: 0.1 M $Na_2B_4O_7$–$H_3BO_3$ buffer solution (pH 7.4) containing 50 mM $K_2S_2O_8$.

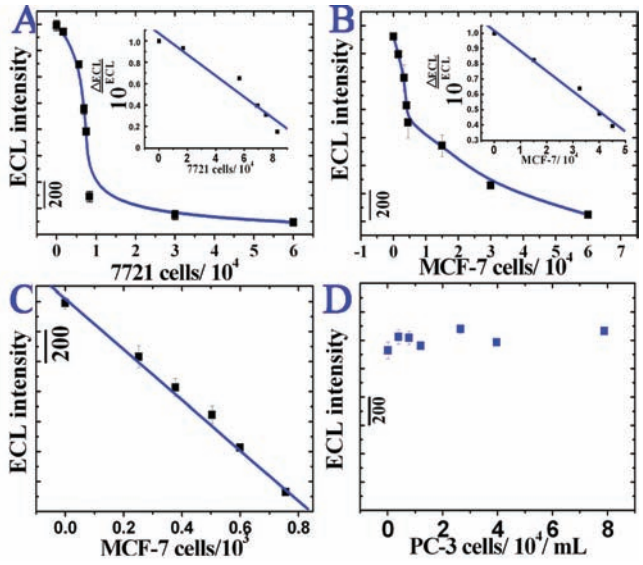


**Figure 4.** The dependence of ECL response on the number of SMMC-7721 cells on the AFP array (A), MCF-7 cells on the CEA array (B), MCF-7 cells on the AFP array (C), and PC-3 cells on the PSA array (D), three measurements for each point. Insets in A and B were the corresponding calibration curves of (ΔECL/ECL) on the number of cells. For different antigen arrays, 0.5 μL of 37.5 ng/mL AFP, 0.5 μL of 71.4 ng/mL CEA, and 0.5 μL of 125 ng/mL PSA were immobilized on each CdS nanorod spot, respectively. ECL-RET signals were recorded at 620 nm. PMT was set at 800 V. ECL detection buffer: 0.1 M $Na_2B_4O_7$–$H_3BO_3$ buffer solution (pH 7.4) containing 50 mM $K_2S_2O_8$.

Finally, we further tested whether each antigen–antibody spots could specifically identify target cells from a mixture of three cell types. Upon incubation with SMMC-7721 cells, MCF-7 cells, and PC-3 cells, the ECL-RET results indicated that a higher signal could be observed at AFP spots for cells mixture than for SMMC-7721 cells and for MCF-7 cells. Also, it can be seen that CEA spots could specifically bind to their corresponding target MCF-7 cells and there were no ECL-RET changes for SMMC-7721 cells and PC-3 cells. These results clearly demonstrated the high selectivity of this detection method which enabled the simultaneous detection of different types of cancer cells from a heterogeneous mixture of cancer cells and required no further labeling of cells.

On the basis of this principle, the amount of proteins on target cells was detected and PSA spots were employed as a negative control. Figure 4A–C showed the quantitative detection results of AFP on SMMC-7721 cells and CEA and AFP receptors on MCF-7 cells. When cells were added into channels, the acceptor's emission at 620 nm decreased gradually with the increasing number of target cells. For SMMC-7721 cells at AFP array (inset in Figure 4A) and MCF-7 cells (inset in Figure 4B) at CEA array, the inhibition of ECL-RET was attributed to the combination of cell surface antigen to $Ru(bpy)_3^{2+}$/antibodies at the antigen array. In this situation, the results showed that $10^{(\Delta ECL/ECL)}$ were proportional to cell concentration (insets in Figure 4A,B). While for MCF-7 cells at the AFP array, ΔECL was directly related to the amount of cell number (Figure 4C). This difference may be due to the different competitive recognition mechanisms. Therefore, antigens on the cell surface could be calculated according to the calibration curve in Figure S6A,B, Supporting Information, and the results in Figure 4A,B. The average antigens on cell surface were 2.3 ± 0.2 ng of AFP for $10^6$ SMMC-7721 cells and 8.8 ± 1.0 ng of CEA for $10^6$ MCF-7 cells, respectively. This result was consistent with Howell's[31] research about CEA in MCF-7 cells (6.2- 9.5 ng/$10^6$ cells), indicating satisfactory accuracy of the competitive ECL-RET immunoassay. Meanwhile, cell counting could be achieved based on the specific combination of cell surface receptors and antigen array. As a control, no ECL changes were observed for PC-3 cells at the PSA spot array (Figure 4D). These results indicated that this on-chip ECL-RET competitive immunoassay can be used not only for multiplexed detection of antigens but also for sensitive detection and identification of various cells simultaneously in a complex matrix.

## CONCLUSIONS

We described a novel method for rapid and multiplexed cancer biomarkers assay based on the mini on-chip ECL-RET competitive immunoassay platform which was testified to be a high-throughput and sensitive strategy. It employed a 64-site antigen/CdS nanorod spot array to realize spatial resolution between adjacent detection locations. The spatial separation of the antigen array allowed an individual ECL-RET immunoassay to be performed at each CdS nanorod spot without interference from cross-talk. On the basis of competitive immune reaction between cell surface antigens and the immunocomplex on the CdS nanorod surface, this microchip device exhibited an excellent identification and quantitative detection of cells in a complex matrix. The presented strategy was demonstrated to be simple and specific and could be applied to other biological assays.

## ASSOCIATED CONTENT

### Supporting Information

Additional information as noted in text. This material is available free of charge via the Internet at http://pubs.acs.org.

## AUTHOR INFORMATION


### Corresponding Author

*Tel/Fax: +86-25-83597294. E-mail: xujj@nju.edu.cn.


### Notes

The authors declare no competing financial interest.

## ACKNOWLEDGMENTS

The work was financially supported by the 973 Program (Grant Number 2012CB932600), the National Natural Science Funds for distinguished Young Scholar (Grant Number 21025522), and the National Natural Science Foundation (Grant No. 20890020, 21135003, 21121091) of China.

## REFERENCES


(1) Song, E. Q.; Hu, J.; Wen, C. Y.; Tian, Z. Q.; Yu, X.; Zhang, Z. L.; Shi, Y. B.; Pang, D. W. *ACS Nano* **2011**, *5*, 761−770.

(2) Tang, J.; Tang, D. P.; Niessner, R.; Chen, G. N.; Knopp., D. *Anal. Chem.* **2011**, *83*, 5407−5414.

(3) Du, D.; Wang, L. M.; Shao, Y. Y.; Wang, J.; Engelhard, M. H.; Lin, Y. H. *Anal. Chem.* **2011**, *83*, 746−752.

(4) Kelloff, G. J.; Boone, C. W.; Crowell, J. A.; Nayfield, S. G.; Hawk, E.; Malone, W. F.; Steele, V. E.; Lubet, R. A.; Sigman, C. C. *J. Cell Biochem. Suppl.* **1996**, *25*, 1−14.

(5) Stoeva, S. I.; Lee, J. S.; Smith, J. E.; Rosen, S. T.; Mirkin, C. A. *J. Am. Chem. Soc.* **2006**, *128*, 8378−8379.

(6) Kim, S. H.; Shim, J. W.; Yang, S. M. *Angew. Chem., Int. Ed.* **2011**, *50*, 1171−1174.

(7) Wilson, M. S.; Nie, W. Y. *Anal. Chem.* **2006**, *78*, 2507−2513.

(8) Du, Y.; Chen, C. G.; Zhou, M.; Dong, S. J.; Wang., E. K. *Anal. Chem.* **2011**, *83*, 1523−1529.

(9) Du, D.; Wang, J.; Lu, D. L.; Dohnalkova, A.; Lin, Y. H. *Anal. Chem.* **2011**, *83*, 6580−6585.

(10) Miao, W. J.; Bard, A. J. *Anal. Chem.* **2003**, *75*, 5825−5834.

(11) Zhang, J.; Qi, H. L.; Li, Y.; Yang, J.; Gao, Q.; Zhang, C. X. *Anal. Chem.* **2008**, *80*, 2888−2894.

(12) Zhang, L. H.; Dong, S. J. *Anal. Chem.* **2006**, *78*, 5119−5123.

(13) Qian, L.; Yang, X. R. *Adv. Funct. Mater.* **2007**, *17*, 1353−1358.

(14) Deiss, F.; LaFratta, C. N.; Symer, M.; Blicharz, T. M.; Sojic, N.; Walt, D. R. *J. Am. Chem. Soc.* **2009**, *131*, 6088−6089.

(15) Sardesai, N. P.; Barron, J. C.; Rusling, J. F. *Anal. Chem.* **2011**, *83*, 6698−6703.

(16) Ding, Z. F.; Quinn, B. M.; Haram, S. K.; Pell, L. E.; Korgel, B. A.; Bard, A. J. *Science* **2002**, *296*, 1293−1297.

(17) Shan, Y.; Xu, J. J.; Chen, H. Y. *Chem. Commun.* **2009**, 905−907.

(18) Zhou, H.; Liu, J.; Xu, J. J.; Chen, H. Y. *Anal. Chem.* **2011**, *83*, 8320−8328.

(19) Wang, J.; Shan, Y.; Zhao, W. W.; Xu, J. J.; Chen, H. Y. *Anal. Chem.* **2011**, *83*, 4004−4011.

(20) Wu, M. S.; Shi, H. W.; Xu, J. J.; Chen, H. Y. *Chem. Commun.* **2011**, *47*, 7752−7754.

(21) Li, L.; Li, M. Y.; Sun, Y. M.; Li, J.; Sun, L.; Zou, G. Z.; Zhang, X. L.; Jin, W. R. *Chem. Commun.* **2011**, *47*, 8292−8294.

(22) Wu, M. S.; Xu, B. Y.; Shi, H. W.; Xu, J. J.; Chen, H. Y. *Lab Chip* **2011**, *11*, 2720−2724.

(23) Kanda, V.; Kariuki, J. K. D.; Harrison, J.; McDermott, M. T. *Anal. Chem.* **2004**, *76*, 7257−7262.

(24) Wang, Z. X.; Lee, J.; Cossins, A. R.; Brust, M. *Anal. Chem.* **2005**, *77*, 5770−5774.

(25) Haab, B. B.; Dunham, M. J.; Brown, P. O. *Genome Biol.* **2001**, *2*, research0004−research0004.13 , DOI: DOI: 10.1186/gb-2001-2-2-research0004.

(26) Nam, J. M.; Thaxton, C. S.; Mirkin, C. A. *Science* **2003**, *301*, 1884−1886.

(27) Zhu, J.; Lu, Y.; Deng, C.; Huang, G. L.; Chen, S. Y.; Xu, S. K.; Lv, Y.; Mitchelson, K.; Cheng, J. *Anal. Chem.* **2010**, *82*, 5304−5312.

(28) Stefanick, J. F.; Kiziltepe, T.; M. Handlogten, W.; Alves, N. J.; Bilgicer, B. *J. Phys. Chem. Lett.* **2012**, *3*, 598−602.

(29) Tsukada, Y.; Bischof, W. K. D.; Hibi, N.; Hirai, H.; Hurwitz, E.; Sela, M. *Proc. Natl. Acad. Sci. U.S.A.* **1982**, *79*, 621−625.

(30) Villacampa, M. J.; Moro, R.; Naval, J.; Failly-Crepin, C.; Lampreave, F.; Uriel, J. *Biochem. Biophys. Res. Commun.* **1984**, *122*, 1322−1327.

(31) Grieve, R. J.; Woods, K. L.; Mann, P. R.; Smith, S. C. H.; Wilson, G. D.; Howell, A. Br. *J. Cancer* **1980**, *42*, 616.

(32) Cavacini, L. A.; Duval, M.; Eder, J. P.; Posner, M. R. *Clin. Cancer Res.* **2002**, *8*, 368−373.